

New airborne pathogen transport model for upper-room UVGI spaces conditioned by chilled ceiling and mixed displacement ventilation: Enhancing air quality and energy performance



Mohamad Kanaan^a, Nesreen Ghaddar^{a,*}, Kamel Ghali^a, Georges Araj^b

^a Department of Mechanical Engineering, American University of Beirut, Beirut, Lebanon

^b Department of Pathology & Laboratory Medicine, American University of Beirut, Beirut, Lebanon

ARTICLE INFO

Article history:

Received 12 April 2014

Accepted 19 May 2014

Available online 12 June 2014

Keywords:

Modeling bacteria transport

UV germicidal irradiation

Air disinfection

Mixed displacement ventilation

Energy efficiency

ABSTRACT

The maximum allowable return air ratio in chilled ceiling (CC) and mixed displacement ventilation (DV) system for good air quality is regulated by acceptable levels of CO₂ concentration not to exceed 700 ppm and airborne bacterial count to satisfy World Health Organization (WHO) requirement for bacterial count not to exceed 500 CFU/m³. Since the CC/DV system relies on buoyancy effects for driving the contaminated air upwards, infectious particles will recirculate in the upper zone allowing effective utilization of upper-room ultraviolet germicidal irradiation (UVGI) to clean return air. The aim of this work is to develop a new airborne bacteria transport plume-multi-layer zonal model at low computational cost to predict bacteria concentration distribution in mixed CC/DV conditioned room without and with upper-room UVGI installed. The results of the simplified model were compared with layer-averaged concentration predictions of a detailed and experimentally-validated 3-D computational fluid dynamics (CFD) model.

The comparison showed good agreement between bacteria transport model results and CFD predictions of room air bacteria concentration with maximum error of ± 10.4 CFU/m³ in exhaust air. The simplified model captured the vertical bacteria concentration distribution in room air as well as the locking effect of highest concentration happening at the stratification level.

The developed bacteria transport model was used in a case study to determine the return air mixing ratio that minimizes energy consumption and maintains acceptable IAQ with and without UVGI. Results showed that the use of upper-room UVGI resulted in 35% in energy saving, whereas the use of in-duct UVGI achieved no more than 12% energy saving, both compared to 100% fresh air case.

© 2014 Elsevier Ltd. All rights reserved.

1. Introduction

Heating ventilation and air conditioning (HVAC) systems is a major contributor to energy consumption in buildings and its contribution is expected to increase in the upcoming years [1]. Therefore, targeting energy cost associated with providing good indoor air quality (IAQ) in HVAC systems is a strategic intervention to reduce building energy consumption [2,3]. A widely used indicator of air quality is the CO₂ concentration level in an air-conditioned room. The CO₂ gas is recognized by ASHRAE (American Society for Heating, Refrigeration and Air conditioning Engineers) as the surrogate ventilation index since it is a good indicator of occupancy and ventilation rate within a space. Although CO₂ by itself is not considered an indoor air contaminant, but it is emitted

by humans who also give off a wide range of 'bioeffluents' which can build up in space, due to poor ventilation [4]. However, in presence of occupants with contagious infections releasing airborne viruses or bacteria, the ventilation requirements might be much higher beyond the requirements for CO₂ concentration to prevent spread of disease. The WHO (1988) [5] recommends not more than 50 CFU of fungi/m³ and a maximum number of bacteria of 100 CFU/m³ of air for hospital environments. In office spaces, the maximum allowable limit of bacterial and fungal count is 500 CFU/m³ [3] although some researchers suggested that the counting of human normal flora bacteria above 200 CFU/m³ air would be considered high [6,7]. This would pose prohibitive ventilation requirement contributing to increased cooling load and energy consumption for hot humid climates. This has led to consideration of other methods that can disinfect air in the duct or in the space which include using ultraviolet germicidal irradiation (UVGI) [8,9] or using high efficient particulate air (HEPA) filters at the

* Corresponding author. Tel.: +961 350000 x2513
E-mail address: farah@aub.edu.lb (N. Ghaddar).

developed analytical two-zone and three-zone mixed models with the air in each zone being fully mixed, but with incomplete mixing between the zones. The mixing coefficients between zones were determined using the inter-zonal velocities found either by measurements or CFD. The model results were compared to CFD values and good agreement was reported for suitable mixing factors.

The main objective of this paper is to develop a multi-layer model for bacteria transport in rooms conditioned by CC/mixed DV system and equipped with upper-room UVGI. The model will predict the maximal return air fraction that can be used to improve the economic viability of the CC/DV system. The use of return air will reduce the effectiveness of this system when the bacterial concentration increases and what would make it worse is the possibility of exhaled stratifications at the breathing level reported by Nielsen et al. [33] as the “locking” of the horizontal exhalation jet. Therefore, the optimal mixing ratio will be the one that minimizes the energy consumption of the system while meeting ASHRAE standard [3] for good indoor air quality and permissible bacteria concentration level recommended by WHO for bacteria count in the breathing zone.

The developed model will be applied on a case study using common infectious bacteria such as *Staphylococcus aureus* [34] which is a bacterium frequently found in the human respiratory tract and on the skin and a known cause of skin infections, respiratory disease and food poisoning. The model will be used as a design tool to determine the effectiveness of the UVGI system and the mixing ratio for maximum energy savings at acceptable indoor air quality and thermal comfort.

2. Mathematical modeling

2.1. The plume multi-zone multi-layer model

In displacement ventilation, the cooler air entering the room at the floor level displaces the warmer room air that rises due to its natural buoyancy effect. Consequently, the bottom occupied zone contains the fresh cool air with no recirculation flow while the heat and contaminants produced by the room activities rise to the ceiling level where they are exhausted. The radiation heat transfer exchange is considered between the occupants and surfaces around them including the inner faces of the walls, and the chilled ceiling. The chilled ceiling carries part of the sensible load by direct radiation and convection [35–37]. The direct and reflected long

wave radiation elements are included in the present model as in Kebabli et al. [38]. Plume multi-layer models of CC/DV conditioned spaces take a physical approach to the problem where the space is divided into horizontal air layers [22,39]. The mass flow in and out of each layer due to heat sources is calculated from the plume equations reported by Mundt [40]. The room is conceptually divided into the following seven air zones (see Fig. 1):

- Zone I: single-layer floor zone where the air is supplied.
- Zone II: multi-layer stratification zone bounded by the stratification height (H_s) and floor zone.
- Zone III: wall plume zone associated with wall buoyant flow.
- Zone IV: multi-layer plume zone from plume virtual source height to the terminal height.
- Zone V: multi-layer air zone outside the plume bounded by H_s and terminal plume height z_t .
- Zone VI: single-layer lower mixed-air zone between z_t and z_{UV} ; and
- Zone VII: single-layer upper mixed-air UV-zone in which air is irradiated.

The interface heights that delimit the zones are the stratification height H_s , plume terminal height z_t , and UV zone height z_{UV} where H_s is the height at which supply flow rate is equal to plume total mass flow rate from sources and from wall (air flow outside the plumes is always upward for below H_s), z_t is the elevation at which the density gradients disappear in the rising air and the plume spreads horizontally, and z_{UV} is the height above which UV-Irradiation is significant. The plume terminal height (z_t) is given by Mundt [40] as follows:

$$z_t = 0.74\Phi^{1/4}(dT/dz)^{-3/8} \quad (1)$$

where Φ is the source heat flux, T is the environment temperature, and z is the vertical coordinate. The stratification height is considered in general as an indicator of good air quality if it is higher than 1.2 m (height of a seated person) where it determines the height of the occupied zone below which CO_2 concentration in air should not exceed 700 ppm [22]. The upper-room UVGI irradiates air in the upper-mixed zone at uniform UV irradiance, E (W/m^2) but does not cover the entire fully-mixed region above the plume terminal height.

The transport equations of bacteria depend on zonal mass and momentum transport of air. Air is supplied at flow rate (\dot{m}_s) at the floor level and moves upward (see Fig. 1). A heat source of

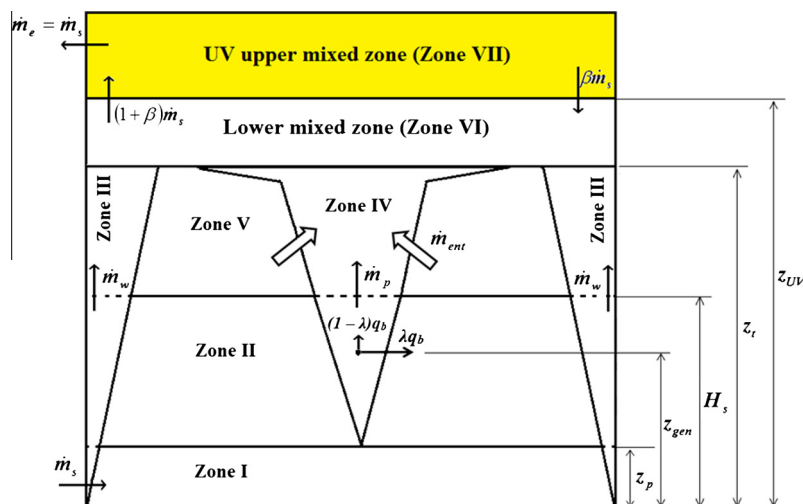


Fig. 1. Schematic of the zonal distribution of DV room equipped with UVGI.

power Φ at height z_p generates an upward plume flow (\dot{m}_p) induced by buoyancy and entrains air flow (\dot{m}_{ent}) from adjacent air zones. In addition, the warm wall induces a wall plume (\dot{m}_w) by entrainment of adjacent room air. Bacteria and CO_2 are generated from occupants at rates q_b and q_o , respectively assuming the breathing mode. The room air moves up until it reaches the stratification height H_s above which it recirculates since the sum of plume flow rates in that zone exceeds the supply flow rate. The zone below the terminal height exchanges recirculation air from the lower-mixing zone. Moreover, inter-zonal air mass flow rate exchanges take place between lower mixed zone and upper UV-zone. The plume flow rates and inter-zonal mass flow rates that will be used in the multi-layer model will be defined in this section. The downdraughts from the chilled ceiling are neglected.

The plume average upward mass flow rate \dot{m}_p is calculated using Mundt correlation [40] as a function of height from the heat source at power Φ and vertical temperature gradient dT/dz of room air as follows:

$$\dot{m}_p = 0.00238\Phi^{3/4}(dT/dz)^{-5/8}B_1 \quad (2b)$$

$$B_1 = 0.004 + 0.039A_1 + 0.38A_1^2 - 0.062A_1^3 \quad \text{and} \\ A_1 = 2.86z(dT/dz)^{3/8}\Phi^{-1/4} \quad (2c)$$

Since the heat source is assumed cylindrical of diameter d and height H_c , it is replaced by a virtual point source such that the border of the plume above the point source passes through the upper edge of the real cylindrical source [41]. The position of the virtual source will be located at $z_0 = 1.8d$ below the actual source [41]. The virtual source will then be located at $z_p = H_c - z_0$ and the vertical distance to be used in the plume flow rate equations (2a and 2b) is $(z - z_p)$. The flow rate of a warm wall plume (\dot{m}_w) is determined from Ayoub et al. [39] multilayer wall-plume model correlations. Even though not all heat sources are bacteria emitting sources, multiple heat sources are lumped into one source of an equivalent heat output and contaminant generation. This approximation would be reasonable since the stratification height is governed by resultant plume flow which is the sum of all single plume flow rates.

The inter-zonal exchanges in the upper region are important for determining bacteria inactivation and their modeling would follow the mixed two-zone model of Noakes et al. [12]. The inter-zonal air flow rate (\dot{m}_{ex}) relative to the absolute room supply flow rate (\dot{m}_s) was defined by Noakes et al. [12] as follows:

$$\beta = \frac{\dot{m}_{ex}}{\dot{m}_s} \quad (3)$$

where β is a dimensionless mixing factor. The inter-zonal flow rate \dot{m}_{ex} is given by

$$\dot{m}_{ex} = \frac{\rho A U_{int}}{2} \quad (4)$$

where A is the interface area and U_{int} is the inter-zonal velocity which can be determined from CFD.

To develop the airborne bacteria transport equations, we follow the model of Ayoub et al. [36] for heat transport in CC/DV conditioned spaces and the multi-layer model of Kanaan et al. [22] for contaminant transport for zones below the terminal height. The multilayer plume model solves the mass and energy balances for air flow and determines the room stratification height and thermal gradient for given supply flow rate, supply temperature and chilled ceiling temperature. The energy balances are not derived here and can be found in [39]. The room supply conditions are determined such that the stratification height is above 1.2 m and temperature gradient does not exceed 2.5 °C/m [19,42].

Fig. 2 shows a schematic of the air and plume layers in the space selected for our analysis. The room is divided to 10 layers. This

number of layers produces grid independent results and the error in numerical results was less than 2% when compared to those obtained for twelve and fourteen layers. The first layer extends from $z = 0$ at the floor level up to the thermal plume virtual source height z_p . The breathing zone is considered to span layers 4 and 5. The bacteria and CO_2 are generated at constant rates in layer 4 that is assigned a small grid height to avoid high concentration gradient at this level and ensure accuracy. Layers 6–8 are equal in height and represent the region between the stratification height and terminal plume height. Layers 9 and 10 represent the two lower and upper zones of the fully-mixed zone previously defined. It is also assumed that the plume terminal height is always below the fully mixed zone. The mathematical model for airborne bacteria transport is presented here based on mass balances for each layer in the different zones and it can predict the bacterial concentration C_b (CFU/m³) in room air and inside plumes, in a typical CC/DV room with the presence of an upper room UV field at uniform-intensity E .

The net circulated flow rate \dot{m}_{cir} at each height z representing the layer height is calculated as

$$\dot{m}_{cir} = \dot{m}_s - \sum_{i=1}^n \dot{m}_{p,i} - \sum_{j=1}^h \dot{m}_{w,j} \quad (5)$$

where n is the number of heat sources and h is the number of hot walls. Assuming control volumes with only one-dimensional inlets and outlets, the steady-state mass balance for Layer 1 is given by

$$\dot{m}_s C_{b,s} + A_1 D \rho \left(\frac{\partial C_b}{\partial z} \right)_1 = \dot{m}_s C_{b,1} \quad (6)$$

In the above equation, $C_{b,s}$ is the airborne bacterial concentration in the supply air stream. The second term on the left side of Eq. (6) is diffusion through the interface of area A_1 with Layer 2, D is the molecular diffusion coefficient of bacteria, and $C_{b,1}$ is the room air bacterial concentration of Layer 1. Diffusion from wall plumes to the room air is neglected since wall plumes are not emitting sources and the difference in contaminant concentration between room air and the wall plume is too slight. In addition, bacteria surface deposition on walls and surfaces are not accounted for in the model due to very small size of bacteria (<2 μm).

The bacteria mass balance for the air layer k ($k = 2-8$) is given by

$$\left(\dot{m}_{cir,k-1} + \sum_{j=1}^h \dot{m}_{w,j,k-1} \right) C_{b,k-1} - A_{int,k} (D + D_t) \rho \left(\frac{\partial C_{b,p}}{\partial r} \right)_{z_{m_k}} \\ + A_k D \rho \left(\frac{\partial C_b}{\partial z} \right)_{z_{m_k}, z_{m_{k-1}}} + \lambda \rho q_{b,k} \\ = \left(\dot{m}_{cir,k} + \sum_{j=1}^h \dot{m}_{w,j,k} \right) C_{b,k} + \dot{m}_{ent,k} C_{b,k} \\ + A_{k-1} D \rho \left(\frac{\partial C_b}{\partial z} \right)_{z_{m_{k-1}}, z_{m_k}} \quad (7)$$

The first term in the left side of Eq. (7) is the convective term associated with air transport and the second term is the diffusion between the plume and adjacent air layer at the middle of that layer. The bacterial concentration inside the plume is $C_{b,p}$, r is the radial coordinate from the plume centerline, \dot{m}_{ent} is the mass entrained by the plume from the adjacent air layer. The molecular diffusion coefficient D is augmented by adding turbulent diffusion coefficient D_t due to the turbulent nature of the plume at its boundaries. This coefficient was correlated to plume upward velocity and characteristic turbulent length that is the plume width at any height [43]. The parameter λ is the fraction of exhaled bacteria that traverse the plume and reach the adjacent room air and $q_{b,k}$ is the volumetric bacteria flow rate generated in layer k where $q_{b,k}$ is q_b for $k = 4$ and zero otherwise. In the current case of exhaled jet of

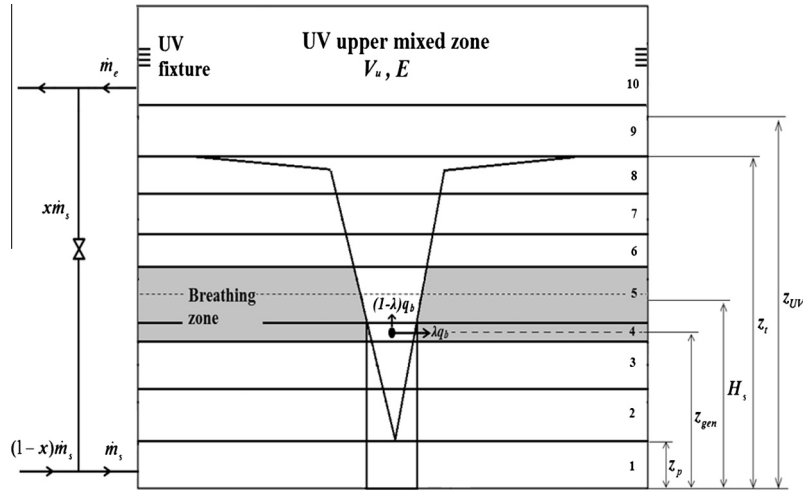


Fig. 2. Schematic of mathematical model with upper UV field.

low velocity, λ can be reasonably assumed zero since the exhaled air is pulled up by the rising thermal plume [44]. In cases of high momentum exhaled flows, the most suitable value of λ can be found by comparing results obtained by the simplified model, at different values of λ , with the CFD simulation to obtain the best fit value.

The bacteria mass balance inside the plume in layer k ($k = 2-8$) is given by:

$$\begin{aligned} & \dot{m}_{p,k-1} C_{b,p,k-1} + \dot{m}_{ent,k} C_{b,k} + (1-\lambda) \rho q_{b,k} \\ & + A_{p,k-1} D \rho \left(\frac{\partial C_{b,p}}{\partial z} \right)_{z_{m_{k-1}}, z_{m_k}} \\ & = \lambda \rho q_{b,k} - A_{int,k} (D + D_t) \rho \left(\frac{\partial C_{b,p}}{\partial r} \right)_{z_{m_k}} \\ & + A_{p,k} D \rho \left(\frac{\partial C_{b,p}}{\partial z} \right)_{z_{m_k} - z_{m_{k+1}}} + \dot{m}_{p,k} C_{b,p,k} \end{aligned} \quad (8)$$

where \dot{m}_p is the mass flow rate of the plume at the boundary and A_p is the plume area at the interface.

The bacteria mass balance in Layer 9 which is the lower mixing zone of the fully-mixed region described previously is given by the following equation where β is the mixing factor defined in Eq. (3):

$$\begin{aligned} & \left(\sum_{j=1}^h \dot{m}_{w,j,8} \right) C_{b,8} + \beta \dot{m}_s C_{b,10} + A_{p,8} D \rho \left(\frac{\partial C_{b,p}}{\partial z} \right)_{z_{m_8}, z_{m_9}} \\ & = (1 + \beta) \dot{m}_s C_{b,9} + A_8 D \rho \left(\frac{\partial C_b}{\partial z} \right)_{z_{m_8}, z_{m_9}} + \dot{m}_{cir,9} C_{b,9} \end{aligned} \quad (9)$$

The bacteria mass balance in the UV upper zone (Layer 10) is given by

$$(1 + \beta) \dot{m}_s C_{b,9} = \beta \dot{m}_s C_{b,10} + \dot{m}_e C_{b,10} + \rho Z E V_u C_{b,10} \quad (10)$$

The term $Z E V_u$ is the UV bacteria inactivation constant where V_u is the volume of the UV upper zone and Z is the bacteria susceptibility to UV. For example, Z is equal to $0.3476 \text{ m}^2/\text{J}$ for the common infectious bacterium *S. aureus* [45].

Ignoring bacteria deposition in return duct and assuming zero concentration of infectious pathogen in outdoor air, the bacterial concentration in the supply air, when a fraction of the return air is used, can then be calculated as

$$C_{b,s} = x C_{b,10} \quad (11)$$

where x is the return mixing ratio.

The linear bacteria transport Eqs. (6)–(11) are discretized using finite difference method. They are solved to find the unknowns: $C_{b,2}$ to $C_{b,10}$ and $C_{b,p,2}$ to $C_{b,p,8}$. The details of the numerical solution methodology used to solve the obtained system of equations were presented in [22]. The developed model accounted for the convection through layers, the diffusion between layers, plumes and room air and it will be validated by detailed CFD simulations. The indoor air quality is assessed based on the bacterial concentration of the room air averaged in the breathing zone for layers 4 and 5 as shown in Fig. 2 and should meet the WHO standard of not to exceed $500 \text{ CFU}/\text{m}^3$ [5].

3. CFD modeling

A detailed CFD model is developed to determine the bacteria distribution in a CC/DV test room. This model can accurately predict the entrainment and mixing between the plume and the surrounding air and can capture the interaction between the upper mixing region and the zone below the plume terminal height. The commercial CFD solver, ANSYS Fluent [46] is used for numerical modeling to solve for the airflow, thermal, and species concentration fields in the room.

3.1. Flow and thermal transport

The room simulation is carried out using a tetrahedral grid containing approximately 127,000 cells ensuring grid independence, refined around the boundaries and species sources. The Reynolds averaged Navier–Stokes equations along with are used to simulate indoor airflow with a uniform measured velocity of 0.15 m/s and corresponding turbulent intensity of 5.5% at the air inlet. A standard $k-\epsilon$ turbulence model is used with enhanced wall treatment and a no slip condition applied at the wall. To account for the thermal buoyancy, the “Boussinesq” approximation is used for the buoyancy-driven flow assuming small density differences in the room air.

All variables, except the pressure, are discretized with the second-order upwind scheme. STANDARD scheme was used for the pressure term and the SIMPLEC scheme with skewness correction 5 is used for coupling pressure and velocity. Numerical convergence is obtained based on many criteria: scaled residuals less than 10^{-5} , net imbalance of mass flow less than 0.5%.

3.2. Bacteria generation and transport

The current simplified model prediction of bacterial vertical concentrations in the occupied zone and upper mixed region will be compared with CFD predicted values of bacteria concentrations averaged for each model layer to evaluate the effectiveness of the upper-room UVGI system in killing one common bacteria type, mainly *S. aureus* [34]. Staphylococci are Gram-positive bacteria with diameters of 0.5–1.5 μm [47] and have a typical mass 10^{-12} g per bacterium [48]. The rate of airborne *S. aureus* from an infected occupant is averaged to be 700 CFU/min assuming breathing mode [49–51]. The transmission of disease caused by *S. aureus* is considered of airborne mode of which the pathogen carriers are droplet nuclei of 1–5 μm [52]. The term “droplet nuclei” was introduced by Wells [53] as being the dried residues of expiratory droplets. In fact, around 90% of particles from human expiratory activities are smaller than 1 μm [54] and then evaporate within a few milliseconds after leaving the mouth by exhalation or coughing and sustain in air for long periods of time [55]. Therefore, it would be reasonable to neglect the settling of pathogens and treat them as gaseous contaminants with low diffusivity (Hathway et al. [28] used a value of 1×10^{-7} kg/m s). The bacteria concentration is then assumed as a passive scalar matter governed by the airflow. The inactivation of microorganisms due to UV irradiation is integrated to the scalar transport equation using Noakes et al. [12] representation as follows:

$$\nabla \cdot (UC) - \nabla \cdot (D\nabla C) - Z \cdot E_p \cdot C = 0 \quad (12)$$

where U is the air velocity field (m/s), E_p is the UV irradiance at a point P in the room. The last term, $Z \cdot E_p \cdot C$, in Eq. (12) is a spatial sink term that represents the rate of inactivation due to the UV field. The boundary conditions of the simulation are listed in Table 1.

The code of the UV irradiation model that predicts field intensity in the whole domain is incorporated to the CFD code in the form of a user-defined function written in programming language C++. The predicted concentrations of the developed bacteria transport plume multi-layer multi-zone model in mixed CC/DV conditioned spaces will be compared to published experimental work of Macher and Miller [56] in which they experimentally investigated the efficacy of upper-room UVGI in inactivating three types of airborne bacteria: *Bacillus subtilis*, *Escherichia coli*, and *Micrococcus luteus* at steady-state conditions.

4. Experimental setup

The CFD model is validated using velocity and temperature measurements made in the experimental CC/DV room at AUB. The supply air temperature and velocity, and wall temperatures are measured and set as boundary conditions for the CFD simulation. Accurate flow and thermal field produced by CFD would result in accurate prediction of bacterial concentration under the assumption that bacteria are airborne and transported with air [12,28].

Fig. 3 shows the schematic of the test room to be used in the simulations. It is a 2.75 m \times 2.5 m \times 2.8 m CC/DV room located in

conditioned space at 24 °C and equipped with UV fixtures for the upper-room UVGI system. The chilled ceiling is composed of three copper tube and plate panels that cover the whole room ceiling area. The chilled water is supplied in parallel to the headers of each panel. The room contains four occupants of which two are infected. Occupants are simulated by heated cylinders of diameter 0.3 m and height 1.2 m each having a heat load of 100 W. Each cylinder has a circular hole of area 1.2 cm² at height 1.05 m that simulates human mouth emitting 0.6 L/min of CO₂ at 34 °C. An anemometer system (Model IFA 300 16 channels, accuracy 0.15%) equipped with a xyz traverse table is used to mount the probes in order to measure air velocity at different points. Temperature is measured using a type T thermocouple linked to the anemometer system. The positions of the thermocouples are shown in Fig. 3. (P: chilled ceiling panel, T: wooden column).

Two 37.5 \times 14 \times 11.2 cm louvered UV fixtures each containing a single 18 W germicidal lamp (Dinies, Germany) are mounted on two opposite walls with centerlines at a height of 2.5 m forming an upper UV irradiated zone of thickness 60 cm [29,53] with bottom is 2.3 m above the floor. Louvers are assumed to be composed of 1 mm thick iron sheets. Reflectors are made of highly reflective stainless Steel of thickness 0.7 mm. A ventilation flow rate of 0.1 kg/s is supplied to the space at measured temperature of 20.44 °C. The chilled ceiling temperature is set at 18.05 °C, which is the average of readings of ten thermocouples mounted on the CC plate (Fig. 3). These conditions are acceptable based on the CC/DV design charts [19] for thermal comfort and indoor air quality. The temperature imposed to room walls in the simulation is the average of three measurements made at the inner surface of three different walls of the test room and it was 22.09 °C.

5. Results and discussion

5.1. Validation of the CFD model

Measured air temperatures and velocities of our current experiment were compared to values obtained from CFD. Table 2 shows a comparison between measured velocities and those obtained from CFD at points of specified coordinates relative to the origin of the room located in the far right corner of the room. Measured and computed velocities show a very good agreement with root-mean-square error of 0.016 m/s. The comparative plot shown in Fig. 4 shows that the temperature measurements and values obtained from CFD agree reasonably with a maximal relative error of 3%.

In order to validate the developed CFD-UV model, the bacteria concentration was predicted for the setup described in the published work of Miller and Macher [56] in which they experimentally measured bacteria concentration and investigated the efficacy of germicidal lamps in reducing airborne bacteria. The scenarios concerned for validating our CFD model applied to Miller and Macher’s room are those with a single unlouvered 15 W UV lamp and constant generation of three culturable bacteria *B. subtilis*, *E. coli*, and *M. luteus*. The average UV irradiance at the breathing level and ceiling level were reported at 0.0069 W/m² and 0.25 W/m² respectively, whereas the values of 0.0084 W/m² and 0.19 W/m² were numerically obtained using our current radiation model. The concentrations of bacterial aerosol at the exhaust [53] reported in colony-forming units, with and without UVGI, were compared with current CFD model results to evaluate the effectiveness of UVGI model at steady-state conditions. The values of UVGI effectiveness using *M. luteus*, *B. subtilis*, and *E. coli* obtained from the CFD model were respectively 0.45, 0.53, and 0.99 that agreed reasonably with the experimental values of 0.49, 0.56, and 1 reported by Miller and Macher [56] at less than 8% error.

Table 1
Boundary conditions used in the simulation.

Room air inflow	$U = 0.15$ m/s, Turbulent intensity: 5.5%, $T = 20.44$ °C
Room air outflow	Pressure outlet
CC temperature	$T = 18.05$ °C, no slip
Room walls	$T = 22.09$ °C, no slip
Heated cylinder	$\Phi = 75$ W, no slip
Mouth	Opening area 1.2 cm ² , $q_b = 700$ CFU/min [50], $q_c = 0.6$ L/min, $T = 34$ °C

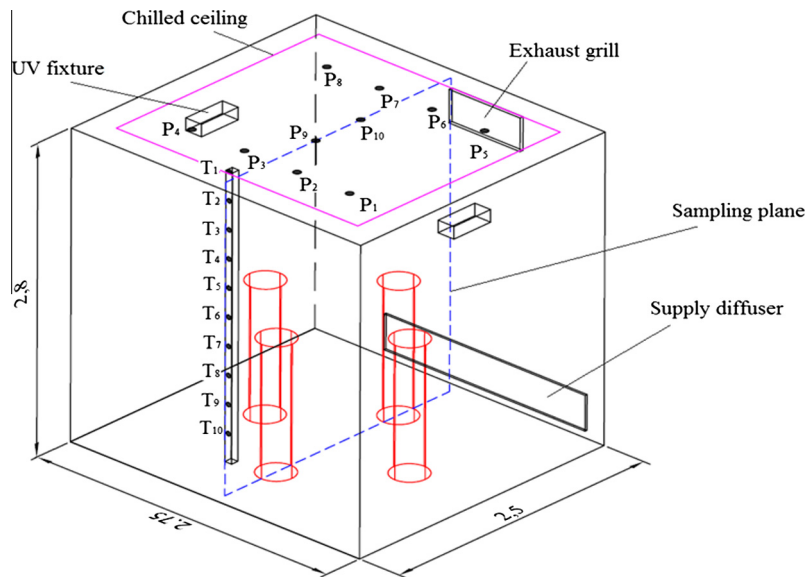


Fig. 3. Schematic of (a) the CC/DV room showing UV fixtures, inflow/outflow boundaries and thermocouple positions.

Table 2
Velocity measurements and values obtained from CFD.

Point	Measured velocity (m/s)	Velocity computed by CFD (m/s)
(109, 143, 70)	0.1367	0.1212
(109, 143, 84)	0.1326	0.1191
(109, 143, 90)	0.1985	0.1771
(109, 143, 103)	0.1663	0.1495
(109, 143, 114)	0.1567	0.1388
(141, 158, 77)	0.1238	0.1104
(141, 158, 55)	0.1386	0.1181
(140, 167, 55)	0.1053	0.0933
(140, 167, 65)	0.1223	0.1057
(140, 167, 100)	0.1118	0.0988

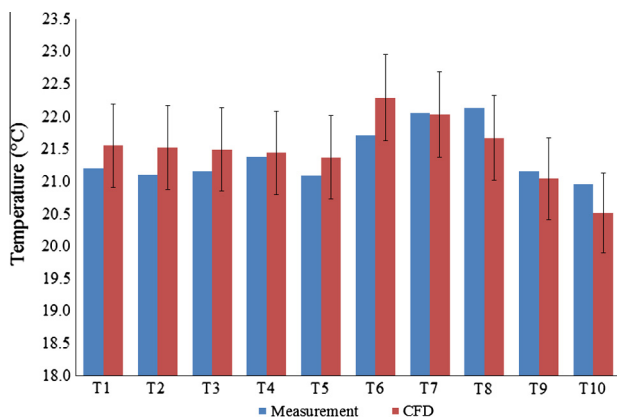


Fig. 4. Comparative plot of measured and CFD values of room air temperature distribution.

5.2. Validation of the bacteria transport plume multi-layer multi-zone model

The comparison of the predicted bacteria concentrations of our new mathematical model to those obtained from CFD are performed for a base case with same load as the experimental room with four occupants of which two are bacteria-emitting fresh DV supply air. To find an equivalent concentration value in CFU/m³ (adopted unit in WHO standard [5]), the molar fraction is

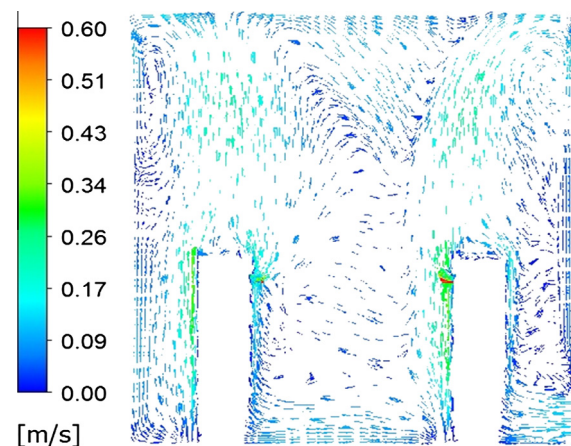


Fig. 5. Velocity vector field predicted by CFD.

multiplied by the bacteria density in kg/m³ and then divided by the mass of one bacterium. The CFU conversion assumes that each colony forming unit arises from a single viable bacterium which is quite conservative in assessing the cleanliness of air. The CFD simulations produced the velocity, temperature, and CO₂ concentration fields as well as bacteria concentration field in molar fraction in the space.

Fig. 5 shows the room velocity vector field on the sampling plane (Fig. 3). The airflow established in the room is almost upward in the lower zone and is re-circulating in the upper zone. The level at which no circulation occurs is the stratification height is at 1.32 m which is sufficiently high to provide thermal comfort and acceptable air quality in the occupied zone.

Temperature and carbon dioxide concentration spatial distributions on the sampling plane are presented in Fig. 6 where two zones can be identified: lower cool and clean zone, and upper warm and CO₂ contaminated separated by the stratification height. The cool air supplied to the room warms due to heat exchange with the heat source and moves upward by buoyancy entraining the contaminant to the upper levels of the room. The room temperature gradient in the room is computed to be about 1.45 °C/m satisfying the thermal comfort condition of a maximal temperature gradient of 2.5 °C/m.

The mass fraction distribution of *S. aureus* when UV device is OFF is shown in Fig. 7 on two horizontal cut planes at (a) height $z = 1.28$ m, (b) height $z = 2$ m. Fig. 7 shows also the bacteria distribution on the vertical sampling plane when (c) UV device is OFF and (d) UV device is ON. The pathogen is transported by the thermal plume around the heat source to the upper levels of the room leaving clean air in the occupied zone. The plots reveal the low diffusion of the bacteria that is much more concentrated in the plume where it is generated and mainly entrained by convection to the upper part of the room. When the upper-room UVGI system is operating, the bacterial concentration decreased significantly in the upper mixed zone and remains almost unchanged in the zone below stratification height.

The multi-layer model predicted the vertical bacteria concentration distribution for room air and in the plume as well as the mixing upper region including the UV zone. Unlike CO_2 transport model [22] where all human sources are emitting sources, bacteria generation is not associated with all heating sources. It is important to ensure that treating all heat sources as single plume source in the bacteria transport model will still predict well the room air bacteria concentration.

The values of bacterial concentration obtained from the simplified model are evaluated as average values for each layer outside the plume from layer 1 to layer 10 and will be compared with bacterial concentrations predicted by the detailed 3-D CFD model averaged over each corresponding layer in the simplified model. The average bacteria concentration will be computed from the CFD model results for each layer volume. The height would represent the mid-layer coordinate z_m .

Fig. 8 compares the multi-layer model and detailed CFD simulation predictions of bacteria concentrations as a function of height for room air (a) without use of UV and (b) while using UV. The simplified multi-layer model captures well the variations and the stratified exhalations due to the flow locking in the temperature gradient [57]. The higher bacteria concentration occurs in the layer of stratification height being the layer receiving both upward and downward mass fluxes through convective transport of bacteria. The CFD model is meant to determine the contaminant concentration in the air surrounding the occupants lumped in the breathing layer and not the concentration in the micro-inhalation zone. The indoor air quality is assessed based on the concentration in the surrounding air that is entrained to inhalation zone of a healthy occupant. It is clear from Fig. 8 that the model results are in good agreement with CFD results with a maximum error of $\pm 34.2 \text{ CFU/m}^3$ in the exhaust air when UV is not used and $\pm 10.4 \text{ CFU/m}^3$ when UV is used.

6. Case study

The validated plume multi-layer multi-zone bacteria transport model is used in a case study to determine which standard is more stringent on the mixing ratio for the CC/DV system; i.e. the CO_2 concentration constraint not to exceed 700 ppm or the bacterial concentration constraint not to exceed 500 CFU/m^3 in the breathing layers. The air quality is assessed in a $5 \text{ m} \times 5 \text{ m} \times 2.8 \text{ m}$ office space in Beirut conditioned by CC/mixed DV during the cooling season. The humidity of the air is assumed to be removed in an economical method using desiccant dehumidifier wheel [58,59] (negligible energy consumption) so that the coil load is only for sensible cooling. The office consists of two external walls (south and west oriented) with two internal partitions and the floor is considered above a conditioned space at 25°C . All the walls have conductance and thermal properties of typical material used in Lebanon and can be found in Refs. [20,22,38]. It is assumed that during the working hours (8:00–13:00, 14:00–18:00), six occupants with three infected are regularly present in the office space. During the lunch hour (13:00–14:00), three occupants with one infected are assumed to remain in the office. The outdoor conditions during operational hours varied between 22°C to 31°C in June, 24°C to 32°C in July, and 24°C to 33°C in August. The load change due to variation in outdoor temperature was small ranging from 4 and 10 W/m^2 . An infectious case is assumed to emit 1400 CFU/min of *S. aureus* by breathing, sneezing, and coughing. The office space is equipped with an upper-room UVGI system consisting of two louvered 12 W UV lamps placed symmetrically on the same wall at an elevation of 2.5 m. We assumed that there is no bacteria growth taking place in the return duct given the constraint of low humidity constrained by the chilled ceiling dew point [60]. Therefore, numerous simulations were performed with and without the use of UVGI to investigate the variations of critical mixing ratio for acceptable CO_2 concentration (not to exceed 700 ppm) and for satisfying the WHO requirement [5] (bacterial concentration not to exceed 500 CFU/m^3) in the occupied zone for different values of stratification height.

6.1. Results without use of UVGI

The variation of critical mixing ratio is shown in Fig. 9 as a function of the stratification height which is strongly correlated with supply airflow rate [19]. The plots show that the critical maximum ratio for good indoor air quality is dictated by the bacteria concentration whose requirement is more restrictive than that of CO_2 concentration. The current office space is simulated for the working

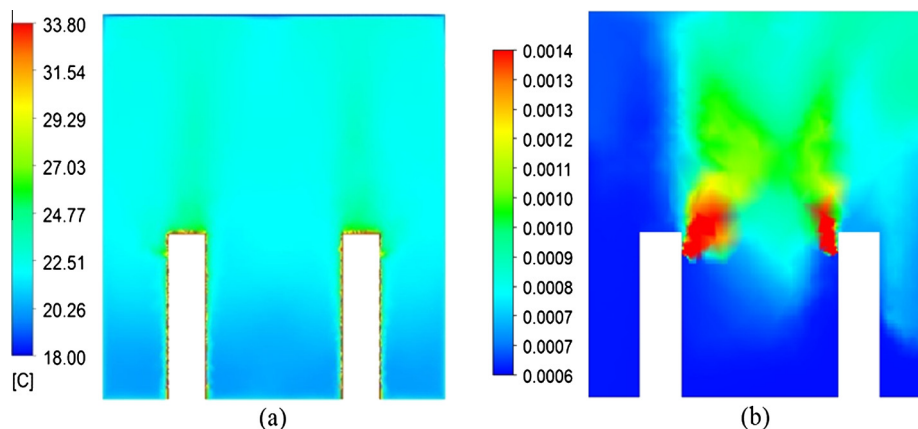


Fig. 6. Predicted results by CFD for (a) Thermal field and (b) CO_2 mass fraction distribution in the room.

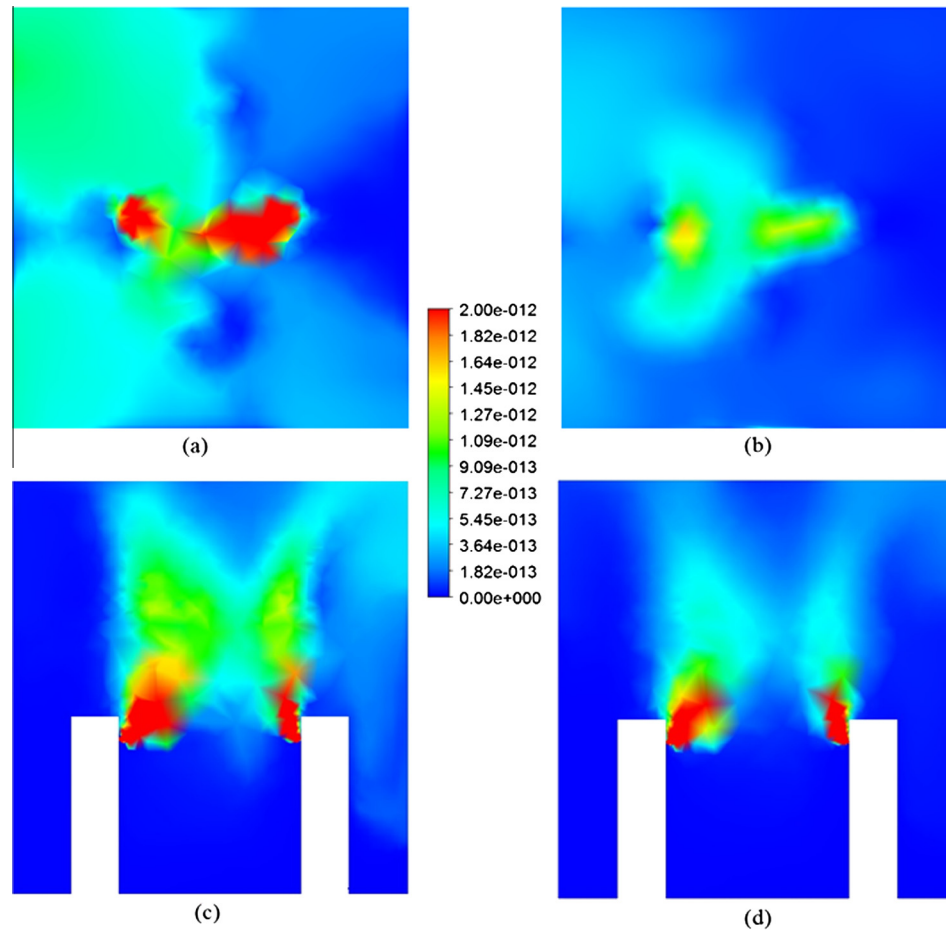


Fig. 7. Contour plots of bacteria mass fraction when UV lamps are OFF on horizontal cut planes at (a) $z = 1.28$ m, (b) $z = 2$ m, and on the sampling plane when UV lamps are (c) ON and (d) OFF.

hours including the peak hour (15:00) and minimum load lunch hour using the analytical model. The supply conditions are determined using the CC/DV charts [19]. The supply flow rate also dictates the allowable mixing ratio for acceptable and healthy indoor air quality. It is shown that during the peak time CO_2 concentration standard limit is obtained for a mixing ratio of 45%, and the corresponding bacteria concentration is 644 CFU/m^3 in the breathing zone. The critical mixing ratio using bacteria concentration standard limit is determined to be 30%. On the other hand, the simulation of the lunch hour shows that a mixing ratio of 42% achieves the 700 ppm CO_2 and results in an acceptable bacteria concentration of 427 CFU/m^3 in the breathing zone.

6.2. Results with the use of UVGI

Since the critical mixing ratio for CO_2 requirement does not satisfy the WHO requirement for bacterial concentration during the peak time, the use of the upper-room UVGI is recommended to reduce the latter to 500 CFU/m^3 without any additional energy consumption on the air conditioning system. In contrary, UVGI is not needed during the lunch hour. The average UV irradiance in the upper zone is predicted using the model of Wu et al. [61] and is found to be 0.13 W/m^2 when the two lamps are ON and 0.07 W/m^2 when only one lamp is ON. The computed average irradiance in the occupied zone is 0.0008 W/m^2 when one lamp is ON and 0.0017 W/m^2 when the two lamps are ON. Both values are below the upper permissible limit of irradiance of 0.002 W/m^2 for human exposure [62,63].

The plume multi-layer multi-zone model is used to simulate the office space for the peak time with the determined critical return ratio of 45% (700 ppm of CO_2 is maintained in the breathing zone) and with the two UV lamps ON. The resulting bacterial concentration in the occupied zone air is reduced to 498 CFU/m^3 compared to the value of 644 CFU/m^3 found when the UV is OFF. A value of 540 CFU/m^3 is found when one lamp is ON. Therefore, the two germicidal lamps with total UV output of 24 W should be operated to obtain the desired level of bacteria concentrations. On the other hand, UV output higher than 24 W will be required to obtain the same air quality if in-duct UVGI is meant to be used due to the short exposure time of air to UV in the supply duct.

The simplified model determined that *S. aureus* killing rate of the in-duct UVGI when used should be about 57% to achieve the 498 CFU/m^3 obtained using 24 W of upper-room UVGI. The required in-duct UV output is estimated to be about 180 W using the work of Lau et al. [64] that experimentally measured the UV irradiance in a similar duct assumed to have same UV reflectance and diffusion properties. The average UV irradiance was about 1.31 W/m^2 which is quite close to the irradiance required in the current case.

The use of upper-room UVGI for reducing bacterial concentrations in occupied spaces is more economical than increasing fresh air intake at the supply. Without the use of the UVGI in the presented case study, the critical mixing ratio of 45% would have been decreased to 30% to establish healthy air quality in the breathing zone. This will result in additional energy consumption on the cooling system while same air quality can be obtained with

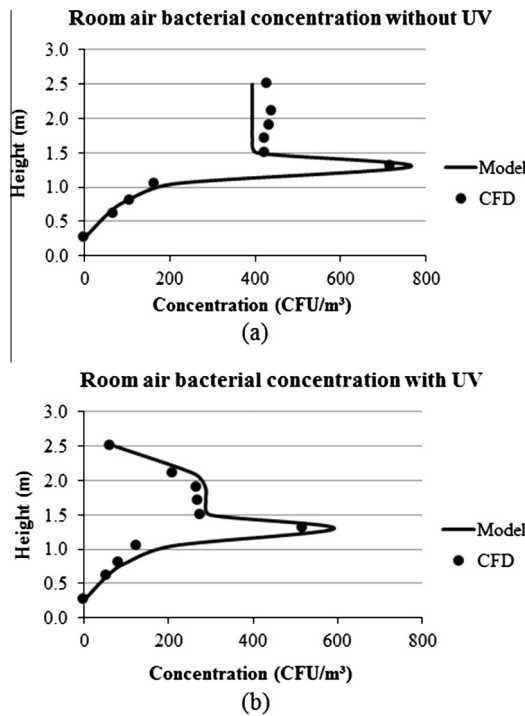


Fig. 8. Plots of bacteria concentration using the multi-layer model and the CFD simulation predictions as a function of height for room air (a) without use of UV lamps and (b) with use of UV lamps.

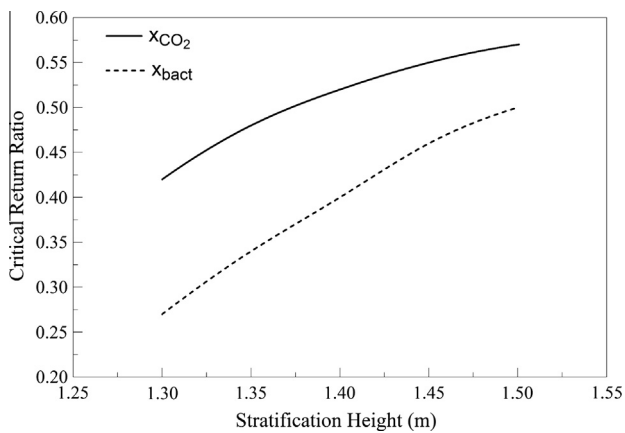


Fig. 9. Variation of critical mixing ratios with stratification height based CO₂ concentration and bacteria concentration standard limits in the occupied zone.

minimum cooling cost using the upper-room UVGI. Fig. 10 shows a comparative plot of the electrical power consumption of the CC/DV system during the peak load on typical days of June (30 °C, 70% RH), July (32 °C, 70% RH), and August (33 °C, 72% RH) for different scenarios. At the peak hour, using the mixing ratio of 30% dictated by the healthy air quality requirement without the use of UVGI, the system consumes 24% less energy than the 100% fresh air system. In presence of UVGI, the return air can be increased to 45% leading to 33% lower energy consumption than the 100% fresh air UVGI is used, while no more than 10% saving is achieved when using in-duct UVGI. The results of the energy simulations over the operational hours of each month are summarized in Table 3 where the daily energy consumption (kWh/day) is provided for conditions that meet IAQ requirements in each case for the months of June, July and August. It is clear that using the return mixing ratio

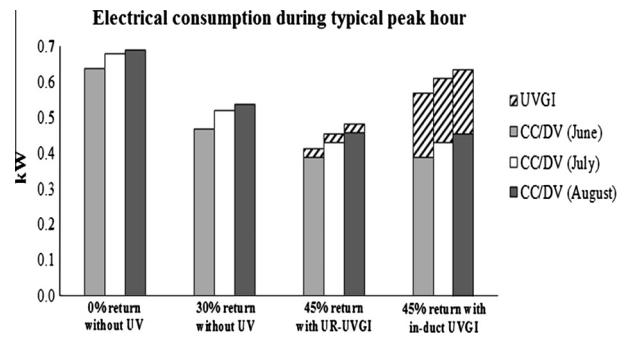


Fig. 10. Comparison of the system electrical consumption during the peak hour on a typical day of June, July and August for different mixing ratios and UVGI types.

Table 3
Daily energy consumption (kW h/day) for conditions that meet IAQ requirements.

Month	100% Fresh supply air	Mixed supply air without UV	Mixed supply air with upper-room UVGI	Mixed supply air with in-duct UVGI
June	6.09	4.46	3.95	5.36
July	6.47	4.92	4.32	5.73
August	6.57	5.11	4.60	6.01

dictated by the WHO standard for bacteria concentrations [5] without the use of UVGI, the system consumes up to 27% less energy than the 100% fresh air system. When the CC/DV uses higher fractions of return air in the presence of UVGI, energy savings can reach 35% in case of upper room UVGI, while no more than 12% saving can be achieved when using in-duct UVGI.

7. Conclusions

A simplified plume multi-layer model has been developed for airborne bacteria transport in rooms conditioned by DV/CC system and equipped with upper room UVGI lowered lamps. The model divided the room into different zones depending on mechanism of bacterial transport for buoyant, partially mixed, and fully mixed regions. The model was validated using CFD simulations and results showed good agreement in predicted bacterial concentrations as function of height using both methods.

The simple bacteria transport model serves as a design tool that can be used to ensure that selected return air ratios in CC/ mixed DV system meets air quality requirements in spaces equipped with upper-room UVGI systems and improve energy performance of the CC/DV system. The use return air in CC/DV rooms enhances the economical viability of this system, but it is constrained by air quality requirements for occupants based on maximum allowable level of bacteria and CO₂ concentrations. It can be concluded from this work that it is the bacteria and not the CO₂ concentration in breathing zone that determines the indoor air quality in CC/DV systems since the CFU count requirement has been proven more restrictive over that of CO₂. The use of upper room UVGI in CC/DV system helps to effectively increase the return mixing ratio and then optimize the energy performance of the system while maintaining good and healthy indoor air quality.

The advantage of mixed DV systems when using upper room UVGI is that the upward airflow in DV systems transports pathogens to the upper irradiated zone where they receive sufficient UV dose due to air recirculation in that zone. The return air is then effectively disinfected before being used with significant fraction in the supply upstream without violating the CFU count

requirement, and at relatively low UV cost when compared to indirect UVGI systems that have less economic viability.

Acknowledgments

The authors would like to thank the Lebanese National Council for Scientific Research (CNRS) for their financial support. The support of the University Research Board (URB) at the American University of Beirut is also acknowledged.

References

- [1] Kharseh M, Altorkmany L, Al-Khawaj M, Hassani F. Warming impact on energy use of HVAC system in buildings of different thermal qualities and in different climates. *Energy Convers Manage* 2014;81:106–11.
- [2] Vakiloroyaya V, Samali B, Fakhar A, Pishghadam K. A review of different strategies for HVAC energy saving. *Energy Convers Manage* 2014;77:738–54.
- [3] Gao CF, Lee WL, Chen H. Locating room air-conditioners at floor level for energy saving in residential buildings. *Energy Convers Manage* 2009;50:2009–19.
- [4] ASHRAE. ANSI/ASHRAE Standard 62.1-2007. Ventilation for acceptable indoor air quality. American society of heating, air-conditioning and refrigeration engineers, Inc.; 2007.
- [5] World Health Organization. Indoor air quality: biological contaminants. World Health Organization, European Series, Copenhagen, Denmark; 1988, p. 31.
- [6] Hood MA. Gram-negative bacteria as aerosols. In: Morey PR, Feeley JC, Otten JA, (editors), Biological contaminants in indoor environments. American Society for Testing and Materials. Philadelphia, Pennsylvania, USA; 1990.
- [7] Morey PR, Chatigny M, Otten J, Feeley J, Burge H, La Force FM, et al. Airborne viable microorganisms in office environments: sampling protocols and analytical procedures. *Appl Indus Hyg* 1986;1:19–23.
- [8] Riley RL, Kaufman JE. Effect of relative humidity on the inactivation of airborne *Serratia Marcescens* by ultraviolet radiation. *Appl Microbiol* 1972;23:1113–20.
- [9] Riley RL, Permutt S, Kaufman JE. Convection, air mixing, and ultraviolet air disinfection in rooms. *Arch Environ Health* 1971;22:200–7.
- [10] First MW. Aging of HEPA filters in service and in storage. *J Am Biol Saf Assoc* 1996;1:52–62.
- [11] ASHRAE Handbook-HVAC Systems and Equipment; 2008.
- [12] Noakes CJ, Beggs CB, Sleight PA. Modeling the performance of upper room ultraviolet germicidal irradiation devices in ventilated rooms: comparison of analytical and CFD methods. *Indoor Built Environ* 2004;13:477–88.
- [13] Bolashikov ZD, Melikov AK. Methods for air cleaning and protection of occupants for airborne pathogens. *Build Environ* 2009;44:1378–85.
- [14] Sung M, Kato S. Method to evaluate UV dose of upper-room UVGI system using the concept of ventilation efficiency. *Build Environ* 2010;45:1626–31.
- [15] Beggs CB, Sleight PA. A quantitative method for evaluating the germicidal effect of upper room UV fields. *J Aerosol Sci* 2002;33:1681–99.
- [16] King MF, Noakes CJ, Sleight PA, Camargo-Valero MA. Bioaerosol deposition in single and two-bed hospital rooms: A numerical and experimental study. *Build Environ* 2012;59:436–47.
- [17] Behne M. Indoor air quality in rooms with cooled ceilings: mixing ventilation or rather displacement ventilation? *Energy Build* 1999;30(2):155–66.
- [18] Ghali K, Ghaddar N, Ayoub M. Chilled ceiling and displacement ventilation system: an opportunity for energy saving in Beirut. *Int J Energy Res* 2007;31:743–59.
- [19] Ghaddar N, Ghali K, Saadeh R, Keblawi A. Design charts for combined chilled ceiling displacement ventilation system. *ASHRAE Trans* 2008;114:574–87.
- [20] Keblawi A, Ghaddar N, Ghali K, Jensen L. Chilled ceiling displacement ventilation design charts correlations to employ in optimized system operation for feasible load ranges. *Energy Build* 2009;41:1155–64.
- [21] Lin B. Simulation study on the energy consumption of displacement ventilation in comparison with mixing ventilation. Proceedings of the International Conference on Energy Conversion and Application (ICECA'2001), p. 1059–1062.
- [22] Kanaan M, Ghaddar N, Ghali K. Simplified model of contaminant dispersion in rooms conditioned by chilled ceiling displacement ventilation system. *HVAC&R Res* 2010;16:765–83.
- [23] Nielsen PV. Analysis and design of room air distribution systems. *HVAC&R Res* 2007;13:987–97.
- [24] Bahman A, Chakroun W, Saadeh R, Ghali K, Ghaddar N. Performance comparison conventional and chilled ceiling/displacement ventilation systems in Kuwait. *ASHRAE Trans* 2009;115:587–94.
- [25] Chakroun W, Ghali K, Ghaddar N. Air quality in rooms conditioned by chilled ceiling and mixed displacement ventilation for energy saving. *Energy Build* 2011;43:2684–95.
- [26] Noakes CJ, Sleight PA, Fletcher LA, Beggs CB. Use of CFD modeling to optimize the design of upper-room UVGI disinfection systems for ventilated rooms. *Indoor Built Environ* 2006;15:347–56.
- [27] Zhu S, Srebric J, Rudnick SN, Vincent RL, Nardell EA. Numerical approach for studying ceiling fan's influence on upper-room UVGI's disinfection efficacy. In: 10th International Conference on Healthy Buildings; 2012. vol. 1. p. 794–799.
- [28] Hathway EA, Noakes CJ, Sleight PA, Fletcher LA. CFD simulation of airborne pathogen transport due to human activities. *Build Environ* 2011;46:2500–11.
- [29] Heidarinejad M, Srebric J. Computational fluid dynamics modeling of UR-UVGI lamp effectiveness to promote disinfection of airborne microorganisms. *World Review of Science, Technology and Sustainable Development*; 2013. 10(1/2/3). p. 78–95.
- [30] Chen C, Zhu J, Qu Z, Lin CH, Jiang Z, Chen Q. Systematic study of person-to-person contaminant transport in mechanically ventilated spaces (RP-1458). *HVAC&R Res* 2014;20:80–91.
- [31] Riley RL, Permutt S. Room air disinfection by ultraviolet irradiation of upper air. *Arch Environ Health* 1971;22:208–19.
- [32] Nicas M, Miller SL. A multi-zone model evaluation of the efficacy of upper-room air ultraviolet germicidal irradiation. *Appl Occup Environ Hyg* 1999;14:317–28.
- [33] Nielsen PV, Jensen RL, Litewnicki M, Zajas JJ. Experiments on the microenvironment and breathing of a person in isothermal and stratified surroundings. 9th International Conference & Exhibition, September 13–17 Syracuse, NY USA; 2009.
- [34] Mandal J, Brandt H. Bioaerosols in indoor environment – a review with special reference to residential and occupational locations. *Open Environ Biol Monit J* 2011;4:83–96.
- [35] Díaz NF. Experimental study of hydronic panels system and its environment. *Energy Convers Manage* 2011;52(1):770–80.
- [36] Díaz NF, Cuevas C. Testing and thermal modeling of radiant panels systems as commissioning tool. *Energy Convers Manage* 2010;51(12):2663–77.
- [37] Ardehali MM, Panah NG, Smith TF. Proof of concept modeling of energy transfer mechanisms for radiant conditioning panels. *Energy Convers Manage* 2004;45(13–14):2005–17.
- [38] Keblawi A, Ghaddar N, Ghali K. Model-based optimal supervisory control of chilled ceiling displacement ventilation system. *Energy Build* 2011;43:1359–70.
- [39] Ayoub M, Ghaddar N, Ghali K. Simplified thermal model of spaces cooled with combined chilled ceiling and displacement ventilation system. *HVAC & R Res* 2006;12:1005–30.
- [40] Mundt E. The performance of displacement ventilation system, Ph. D thesis. Sweden: Royal Institute of Technology; 1996.
- [41] Goodfellow HD. Industrial ventilation design guidebook. A Harcourt Science and Technology Company, San Diego, California, USA; 2001.
- [42] Mossolly M, Ghaddar N, Ghali K, Jensen L. Optimized operation of combined chilled ceiling displacement ventilation system using genetic algorithm. *ASHRAE Trans* 2008;114:541–54.
- [43] Chen Q, Xu W. A zero-equation turbulence model for indoor airflow simulation. *Energy Build* 1998;28:137–44.
- [44] Russo JS, Khalifa E. Computational study of breathing methods for inhalation exposure. *HVAC&R Res* 2011;17:419–31.
- [45] Sharp DG. The effects of ultraviolet light on bacteria suspended in air. *J Bacteriol* 1940;39:535–54.
- [46] ANSYS Software. ANSYS© 2010. <<http://www.ansys.com>>.
- [47] Harris LG, Foster SJ, Richards RG. An introduction to *Staphylococcus aureus*, and techniques for identifying and quantifying *S. aureus* adhesion to biomaterials: review. *Eur Cells Mater* 2002;4:39–60.
- [48] Davis, Dulbecco, Eisen, Ginsberg, Bacterial Physiology: Microbiology, Second Edition, Maryland: Harper and Row; 1973. p. 96–97.
- [49] Xu Z, Shen F, Li X, Wu Y, Chen Q. Molecular and microscopic analysis of bacteria and viruses in exhaled breath collected using a simple impaction and condensing method. *PLoS ONE* 2012;7:e41137. <http://dx.doi.org/10.1371/journal.pone.0041137>.
- [50] Singh P, Mahajan RP, Murty GE, Aitkenhead AR. Relationship of peak flow rate and peak velocity time during voluntary coughing. *Br J Anaesth* 1995;74:714–6.
- [51] Gupta JK, Lin CH, Chen Q. Characterizing exhaled airflow from breathing and talking. *Indoor Air* 2010;20:31–9.
- [52] Wan MP, Chao CYH, Ng YD, Sze To GN, Yu WC. Dispersion of expiratory droplets in a general hospital ward with ceiling mixing type mechanical ventilation system. *Aerosol Sci Technol* 2007;41:244–528.
- [53] Wells WF. On air-borne infection. Study II. Droplets and droplet nuclei. *Am J Hyg* 1934;20:611–8.
- [54] Papineni RS, Rosenthal FS. The size distribution of droplets in the exhaled breath of healthy human subjects. *J Aerosol Med: Deposition, Clearance, Effects Lung* 1997;10:105–16.
- [55] Morawska L. Droplet fate in indoor environments, or can we prevent the spread of infection? *Indoor Air* 2006;16:335–47.
- [56] Miller SL, Macher JM. Evaluation of a methodology for quantifying the effect of room air ultraviolet germicidal irradiation on airborne bacteria. *Aerosol Sci Technol* 2000;33:274–95.
- [57] Nielsen PV, Olmedo I, Ruiz de Adana M, Grzelecki P, Jensen RL. Airborne cross-infection risk between two people standing in surroundings with a vertical temperature gradient. *HVAC&R Res* 2012;18:552–61.
- [58] Beccali M, Butera F, Guanella R, Adhikari RS. Simplified models for the performance evaluation of desiccant wheel dehumidification. *Int J Energy Res* 2003;27:17–29.
- [59] She X, Yin Y, Zhang X. Thermodynamic analysis of a novel energy-efficient refrigeration system subcooled by liquid desiccant dehumidification and evaporation. *Energy Convers Manage* 2014;78:286–96.

- [60] Yau YH, Ng WK. A comparison study on energy savings and fungus growth control using heat recovery devices in a modern tropical operating theatre. *Energy Convers Manage* 2011;52(4):1850–60.
- [61] Wu CL, Yang Y, Wong SL, Lai ACK. A new mathematical model for irradiance field prediction of upper-room ultraviolet germicidal systems. *J Hazard Mater* 2011;189:173–85.
- [62] American Conference of Governmental Industrial Hygienists. TLVs and BEIs. Cincinnati: ACGIH; 1999.
- [63] Nardell EA, Bucher SJ, Brickner PW, Wang C, Vincent RL, Becan-McBride K. Safety of upper-room ultraviolet germicidal air disinfection for room occupants: results from the tuberculosis ultraviolet shelter study. *Public Health Rep* 2008;123:52–60.
- [64] Lau J, Bahnfleth W, Mistrick R, Kompore D. Ultraviolet irradiance measurement and modeling for evaluating the effectiveness of in-duct ultraviolet germicidal irradiation devices. *HVAC&R Res* 2012;18:626–42.